Molecular Vision 2021; 27:221-232 <http://www.molvis.org/molvis/v27/221>
Received 19 December 2020 | Accepted 5 May 2021 | Published 7 May 2021

Clinical characterization and the improved molecular diagnosis of autosomal dominant cone-rod dystrophy in patients with SCA7

Xuan Zou,[1] Fengxia Yao,[2] Fengrong Li,[3] Shijing Wu,[1] Hui Li,[1] Zixi Sun,[1] Tian Zhu,[1] Xing Wei,[1] Donghui Li,[1] Ruifang Sui[1]

(The first two authors contribute equally to this paper.)

[1]Department of Ophthalmology, Peking Union Medical College Hospital, Chinese Academy of Medical Sciences & Peking Union Medical College, Beijing, China; [2]Medical Research Center, Peking Union Medical College Hospital, Chinese Academy of Medical Sciences & Peking Union Medical College, Beijing, China; [3]Department of Ophthalmology, Beijing Hospital of Traditional Chinese Medicine, Capital Medical University, Beijing, China

Purpose: To evaluate the retinal phenotype and genetic features of Chinese patients with spinocerebellar ataxia type 7 (SCA7).

Methods: Detailed ophthalmic examinations, including electroretinograms, fundus photography, fundus autofluorescence and optical coherence tomography, were performed to analyse the retinal lesions of patients with SCA7. A molecular genetic analysis was completed to confirm the number of CAG repeats in *ATXN7* gene on the patients and their family members.

Results: Eight patients from three families with SCA7 were included in this study. Trinucleotide repeat was expanded from 43 to 113 in the affected patients. The affected patients were characterized by different degrees of cone-rod dystrophy, which is positively related to the number of CAG repeats and age. All patients complained of progressive bilateral visual loss, and most cases reported visual disturbance earlier than gait movement or dysarthria. A coarse granular appearance of the macular region on scanning laser ophthalmoscopy, hypofluorescence in the macula on autofluorescence, retinal atrophy on optic coherence tomography, depression of multifocal electroretinograms and prominent abnormalities in cone-mediated responses on electrograms are the general features of SCA7-related retinopathy. Hyperreflective dots in the outer retinal layers and choroidal vessel layers are a common sign in optic coherence tomography in the advanced stage.

Conclusions: SCA7 shows a cone-rod dystrophy phenotype. The multimodal imaging of the retina is beneficial to detect the early lesions of cone-rod dystrophy related to SCA7.

Spinocerebellar ataxias (SCAs) are a genetically diverse group of autosomal dominant disorders primarily characterized by degeneration of the cerebellum, brainstem, and spinal cord [1,2]. Although these disorders have different clinical features and disease-causing genes, SCAs all share a common underlying mutational mechanism: an expanded CAG repeat encoding a tract of glutamine amino acids (polyglutamine or polyQ tract). Visual system involvement is one of the clinical features of SCAs, and it may be the presenting sign for some types of SCAs. Specifically, the ocular motor features of SCAs include impaired saccadic velocity, impaired smooth pursuit gain, deficits in the vestibulo-ocular reflex, and nystagmus. Optic nerve atrophy and retinal degeneration have also been described in certain types of SCAs [3-5].

Correspondence to: Ruifang Sui, Department of Ophthalmology, Peking Union Medical College Hospital, 1 Shuai Fu Yuan, Beijing 100730, China; Phone: +86-10-69156361; FAX: +86-10-69156361; email: hrfsui@163.com

Spinocerebellar ataxia type 7 (SCA7; OMIM:164500) is caused by the expansion of a CAG triplet repeat that is translated into a polyglutamine tract in ataxin-7 (*ATXN7,* NM_000333, OMIM: 607640). SCA7 is clinically distinguished from other types of SCAs by the additional presence of retinal degeneration. The ophthalmic features of SCA7 are progressive visual disturbance mainly due to retinal degeneration and impaired ocular motility [6], which produces a specific diagnosis. Presenting visual symptoms may include photophobia, dyschromatopsia, decreased vision, and hemeralopia [7]. The appearance of the fundus in SCA7 is variable, and the reported phenotypes range from normal appearance to occult macular dystrophy (OMD), macular dystrophy, and cone-rod dystrophy (CORD) [1,8-11]. Ocular motor abnormalities may include slowed saccades, saccadic pursuits, saccadic dysmetria, and gaze-evoked nystagmus [7], which are relatively non-specific for olivopontocerebellar atrophies. Decreased corneal endothelial cell density and increased corneal thickness have also been reported [2].

There have been several reports on the visual disturbances in *AXTN7*-associated retinopathy [1,8-11]. However, there are limited data on the ophthalmic clinical spectrum and genetics of SCA7 in the Chinese population. To complement and extend these investigations, we characterized the retinal function and structure in detail for patients from three families with SCA7.

METHODS

Patients: Eight patients from three families with SCA7 were included in this study (Figure 1). All participants were identified at the Ophthalmic Genetics Clinic at Peking Union Medical College Hospital (PUMCH), Beijing, China. The patient cohort included 6 male patients and 2 female patients. The age of the patients ranged from 4 to 57 years, and the median age was 32 years. Family members were identified as affected by family history or genetic testing or both. Written informed consent was obtained from either the participating individuals or their guardians. This study was approved by the Institutional Review Board of PUMCH (No. JS-2059) and adhered to the tenets of the Declaration of Helsinki, the Guidance on Sample Collection of Human Genetic Diseases by the Ministry of Public Health of China, and the ARVO statement on human subjects.

Clinical evaluation: A complete medical history and family history of each participant were obtained. The clinical

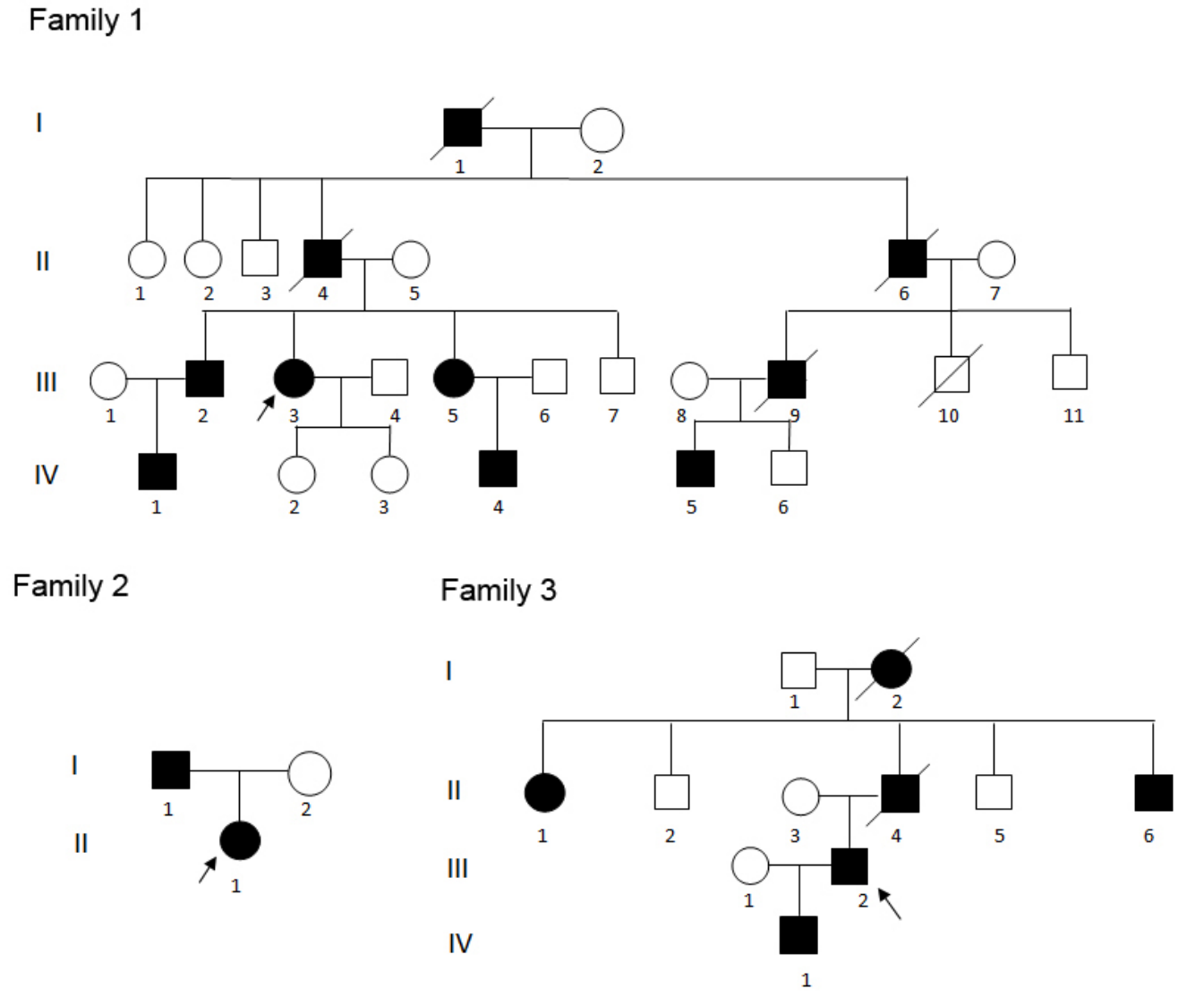

Figure 1. Pedigrees of families with variants in *AXTN7*. The circles represent females, and the squares represent males. The black symbols denote the individuals affected with SCA7. The arrow indicates the proband. The slashed symbols indicate deceased members.

evaluation included measurements of the best-corrected decimal visual acuity (BCVA), ophthalmoscopy, fundus photography (Topcon, Tokyo, Japan, or HFC, Micro Clear Medical, Suzhou, China), imaging of fundus autofluorescence (FAF), and 633-nm laser of a scanning laser ophthalmoscope (SLO; Heidelberg Engineering, Heidelberg, Germany), optical coherence tomography (OCT; Topcon, Tokyo, Japan, or Heidelberg Engineering), and visual field (VF) testing (Haag-Streit, Koeniz, Switzerland). Electroretinogram (ERG) was recorded according to the standards of the International Society for Clinical Electrophysiology of Vision (RetiPort ERG System; Roland Consult, Wiesbaden, Germany or The RETeval device; LKC, Gaithersburg, MD) [12]. Multifocal ERGs (VERIS, EDI Inc., Milpitas, CA) were also recorded when possible.

Molecular analyses: Genomic DNA was isolated from peripheral leukocytes using a QIAamp DNA Blood Midi Kit (Qiagen, Hilden, Germany) according to the manufacturer's protocol. A locus-specific FAM fluorescently labeled forward primer (5′-FAM-TGT TAC ATT GTA GGA GCG GAA-3′) was designed, and the reverse primer was the no-labeled sequence (5′-CAC GAC TGT CCC AGC ATC ACT T-3′). PCR was performed in 25 µl reaction volumes containing 20–100 ng genomic DNA, 10 µM of each primer, the 2X KAPA HiFi HotStart PCR Kit (Kapa Biosystems, Cape Town, South Africa), and double-distilled water (ddH_2O). Initial denaturation was at 95 °C for 5 min, followed by amplification for 35 cycles with denaturation at 95 °C for 45 s, annealing at 55 °C for 50 s, and extension at 72 °C for 60 s. A total of 1 µl of the reaction products was added to 12 µl of Hi-Di formamide and 0.5 µl GeneScan 500 LIZ Size Standard (Applied Biosystems , Warrington, UK), denatured at 95 °C for 2 min, and immediately placed on ice for a minimum of 3 min. The samples were injected in an ABI 3500xL Genetic Analyzer with a 50 cm capillary containing POP7. The amplicon length was calculated in comparison with the GeneScan 500 LIZ with the GeneMarker V1.5 demo program.

To precisely assess the number of CAG repeats, one healthy control with two homozygous controls was Sanger-sequenced. Sanger sequencing was performed using the BigDye Terminator Cycle Sequencing Ready Reaction Kit version 3.1 (Applied Biosystems, Thermo Fisher Scientific, Inc., Waltham, MA), and the sequence was analyzed with an ABI Prism 3130 automated sequencer. The sequencing results were compared against the reference genomic sequence obtained from the University of California, Santa Cruz (Santa Cruz, CA) Genome Browser (*ATXN7,* NM_000333). Twenty-five healthy controls were tested to calculate the allele frequencies in the Chinese population.

To determine the exact number of CAG repeats for each tested sample and obtain the standard profile of a homozygous individual, one homozygous genotype was selected. The healthy homozygous control with Sanger sequencing and capillary electrophoresis fragment analysis contained 10 CAG repeats, and the corresponding length was 294 bp. Thus, the number of CAG repeats was [the length -(294–30)]/3.

Case reports:

Family 1:

Family 1 Case III:3—A 54-year-old woman noticed decreased visual acuity and mild photophobia at age 45. Gait disturbance and dysarthria occurred at age 51. Brain magnetic resonance imaging (MRI) demonstrated mild cerebellar atrophy. When she consulted us, her BCVA was 0.1 OU with a refraction of +1.50 × 60 OD and +1.0 × 100 OS. Intraocular pressure was 11 mmHg in both eyes. Nystagmus was not detected. The slit-lamp biomicroscopic examination showed that the anterior segments were unremarkable. The fundus photography showed coarse granular depigmentation in the macular area (Figure 2A,B), which corresponded with a round hypofluorescence patch with a surrounding hyperfluorescent ring on FAF (Figure 3A,B). OCT revealed a disorganized retinal structure in the macula, thinning of the RPE, and the absence of an ellipsoid zone and an outer limiting membrane. Multiple hyperreflective dots above and beneath the retinal RPE layer were detected. A mild epiretinal membrane formed in the left eye (Figure 4A–D). A coarse granular appearance of the macula was observed with the SLO (Figure 5A,B). VF analysis showed a central scotoma in both eyes. The ERGs showed severely decreased cone responses and relatively normal rod function (Figure 6). Multifocal ERGs demonstrated a depression of the response amplitude in the macular area. The CAG repeat sequences in *ATXN7* were extended to 45.

Family 1 Case IV:5—A 32-year-old man, the nephew of Case III:3, complained of blurred vison and photophobia at age 26 and gait disturbance and dysarthria at age 30. Computed tomographic scans and magnetic resonance images showed atrophy in the cerebellar region. His BCVA was 0.4 OD and 0.32 OS. His eye movements were full without nystagmus. The slit-lamp biomicroscopic examination revealed that the anterior segment was normal in both eyes. The fundus showed macular atrophy with surrounding pigment changes (Figure 2C,D) similar to those of Case III:3. The ERGs demonstrated severely decreased cone responses and preserved rod function. The number of CAG repeats in *ATXN7* was 50.

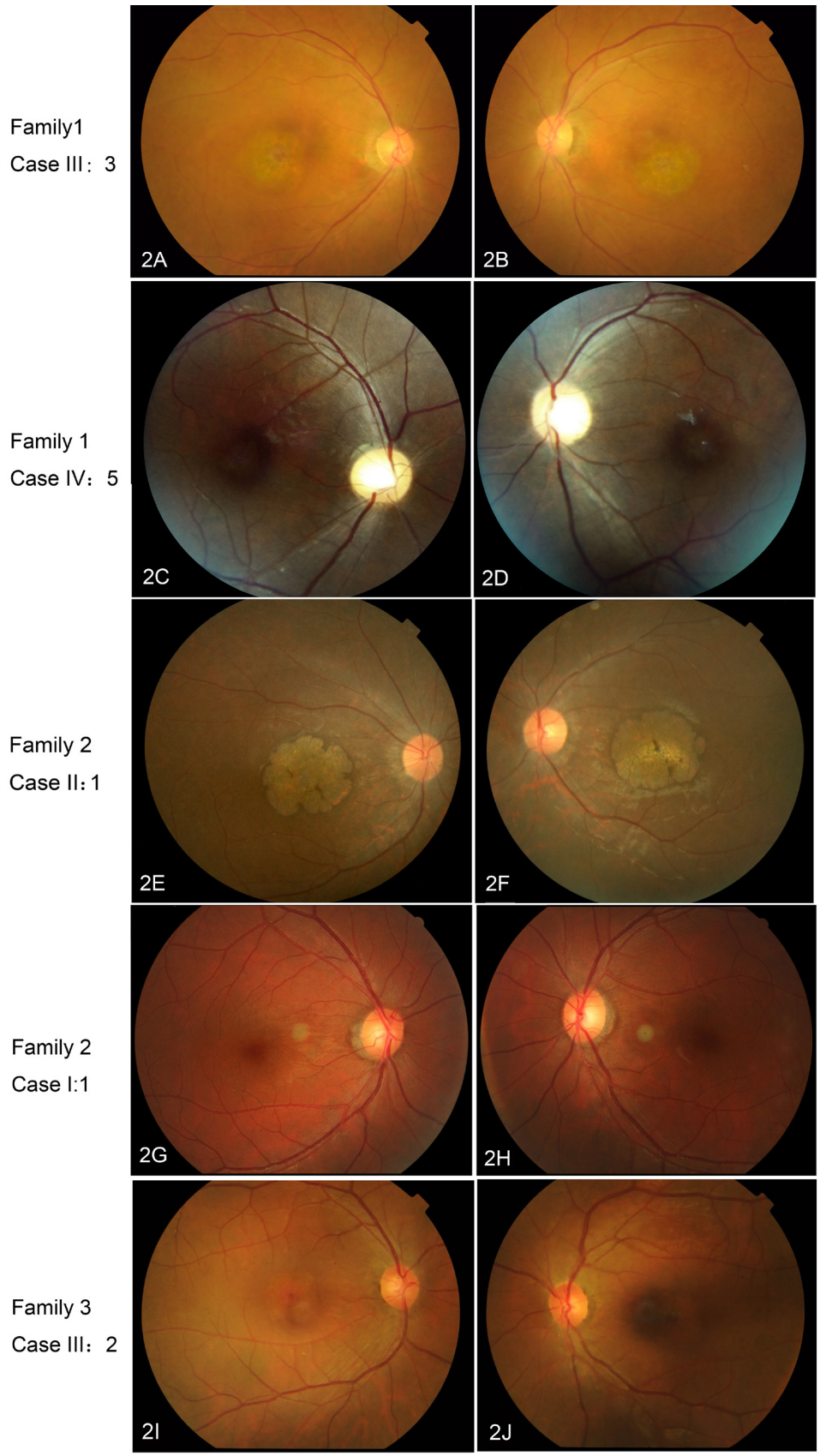

Figure 2. Fundus photographs of patients with variants in *AXTN7*. **A**, **B**: Family 1 Case III:3 is a 54-year-old woman. The fundus shows obvious macular atrophy. **C**, **D**: Family 1 Case IV:5 is a 32-year-old man. The fundus also shows obvious macular atrophy. **E**, **F**: Family 2 Case II:1 is a 14-year-old girl. The fundus shows about two disc-sized atrophic lesions in a petal-like shape with surrounding pigment changes. **G, H**: Fundus photographs taken during the second visit of Family 2 Case I:1 when he was 42 years old. The fundus shows a relatively normal appearance. **I**, **J**: Family 3 Case III:2 is a 32-year-old man. The fundus shows obvious macular atrophy.

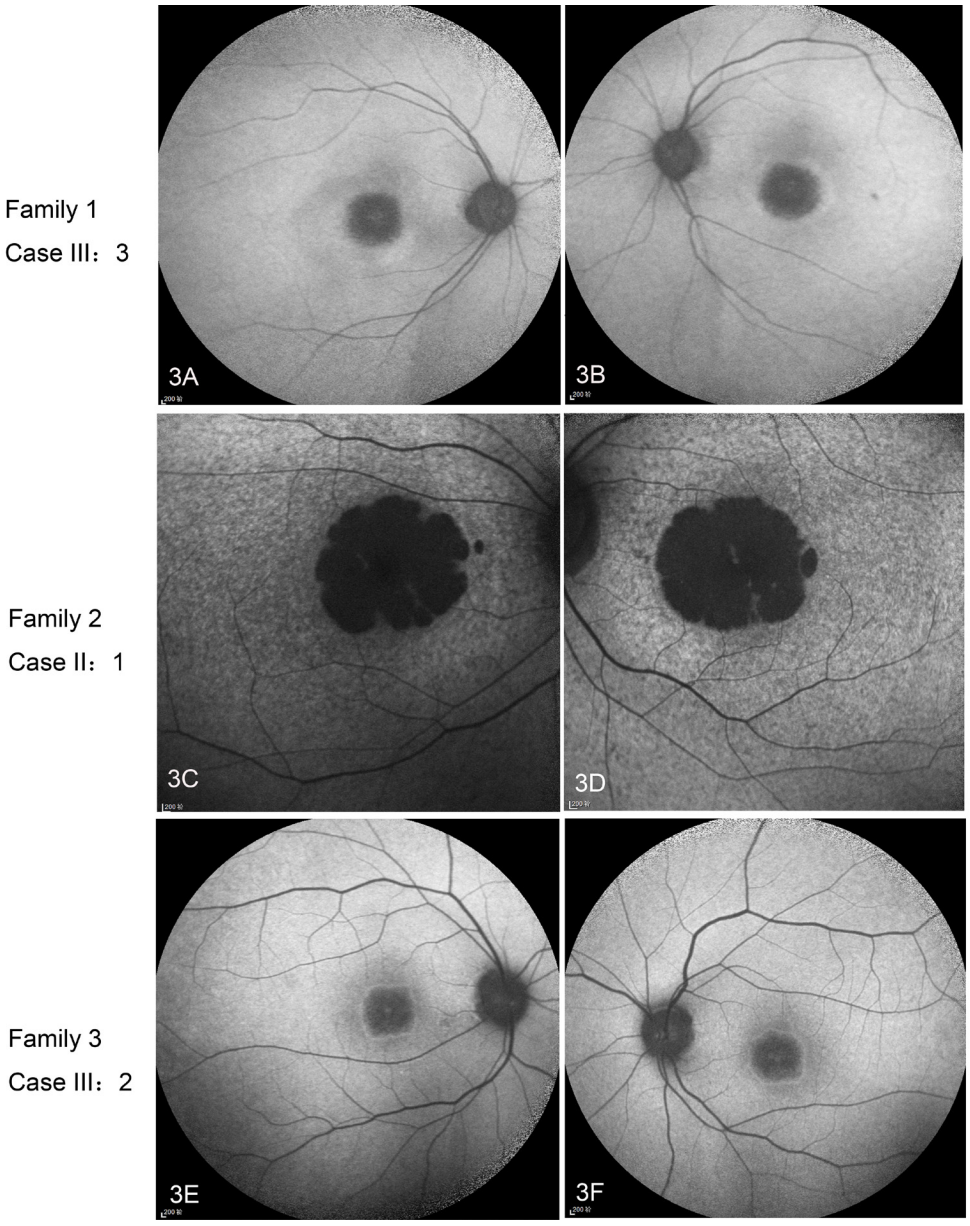

Figure 3. AF in patients with variants in *AXTN7*. **A**, **B**: Family 1 Case III:3 is a 54-year-old woman. Autofluorescence (AF) shows a hypofluorescence patch in the macular area with a surrounding hyperfluorescent ring. **C**, **D**: AF was taken during the second visit of Family 2 Case II:1 when she was 18 years old. AF shows a dark macula and mottled fluorescence in the posterior pole. **E**, **F**. Family 3 Case III:2 is a 32-year-old man. AF shows a hypofluorescence patch in the macular area with a surrounding hyperfluorescent ring.

Other Family 1 affected members: Two other family members were affected, and they were confirmed with genetic testing without an ophthalmic examination. Case III:9, a 57-year-old man, noticed gait disturbance, dysarthria, and decreased visual acuity in his 40s. He was wheelchair-bound, and vision was hand motion in both eyes. He was deceased at the age of 58. The CAG repeat sequences in *ATXN7* were extended to 43. Case IV:4, a 26-year-old man, had blurred vision in his teenage years and gait disturbance and dysarthria at age 18. He had been paralyzed and had no light perception in both eyes for about six years. He had the most severe symptoms in Family 1. The number of expanded CAG repeats was 56.

Family 2: A 14-year-old girl (Case II:1) presented with decreased visual acuity at age 12 and gait disturbance at age 13. Brain MRI revealed a mild volume loss in the cerebellum. Her BCVA was 0.1 OD with a refraction of −1.0−1.0 × 3 and 0.08 OS with a refraction of −1.75 at the first visit. The anterior segments were normal. The fundus showed about two disc-sized atrophic lesions in a petal-like shape with surrounding pigment changes (Figure 2E,F), and FAF showed a hypofluorescent macula and mottled fluorescence in the posterior pole (Figure 3C,D). OCT showed a preserved laminar retinal structure in the macula, thinning of the RPE, and absence of an ellipsoid zone and an outer limiting

membrane. In addition, there were a few hyperreflective dots in the outer layers of the retina (Figure 4E–H). VF analysis indicated a central scotoma in both eyes. The ERGs revealed severely decreased cone responses with limited preserved rod function. The patient's ERGs became non-recordable (Figure 6), and her BCVA decreased to 0.04 (OD) and 0.03 (OS) 3 years later during a follow-up visit. The CAG repeat sequence in *ATXN7* was extended to 62.

Her father (I:1) did not have a vision complaint and showed a normal OCT structure (Figure 4I,J) when he first visited us at age 38 to accompany his daughter. His ERGs were normal in the dark- and light-adapted responses (Figure 6). One year later, he began to notice gradually decreasing visual acuity. He was genetically confirmed by the expanded 45 CAG repeats. He consulted us again at age 42 with a BCVA of 0.1 OU with a refraction of −0.75 × 80 OD and

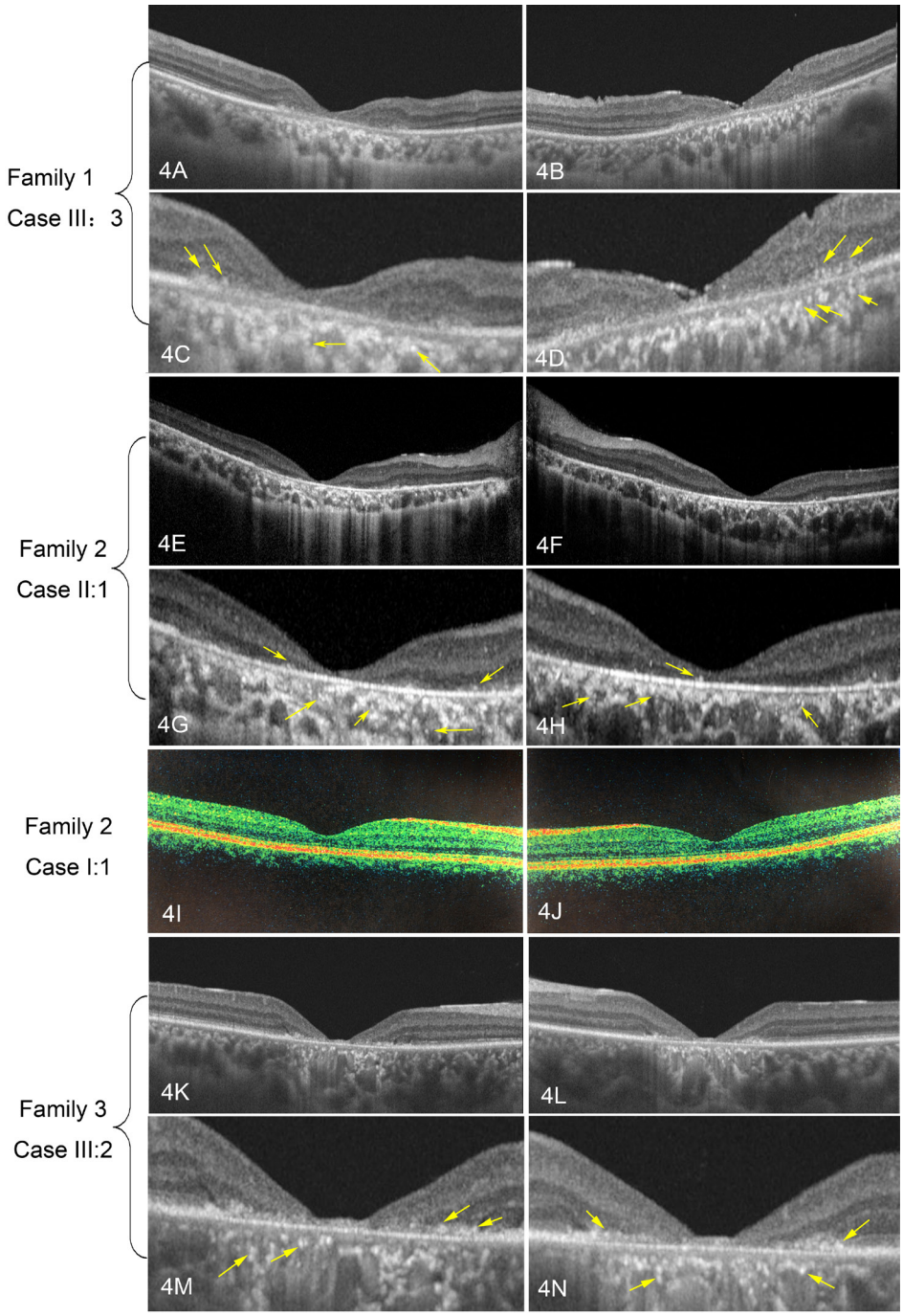

Figure 4. Optical coherence tomography (OCT) of patients with variants in *AXTN7*. Family 1 Case III:3 (a 54-year-old woman; **A–D**), Family 2 Case II:1 (an 18-year-old girl during the second visit; **E–H**), and Family 3 Case III:2 (a 32-year-old man; 4 K-4N) have a similar appearance. Optical coherence tomography (OCT) shows thinning of the macula, with the outer layers and retinal pigment epithelium (RPE) affected more severely. The ellipsoid zone disappears in the fovea area, indicating the appearance of cone-rod dystrophy (CORD). There are many intra-retinal hyperreflective dots, which are indicated by the yellow arrows. Panels **C** and **D** are enlargements of panels **A** and **B**, panels **G** and **H** are enlargements of panels **E** and **F**, and panels **M** and **N** are enlargements of panels **K** and **L**. Family 2 Case I:I (**I** and **J**) showed a normal OCT when he first consulted us at age 38.

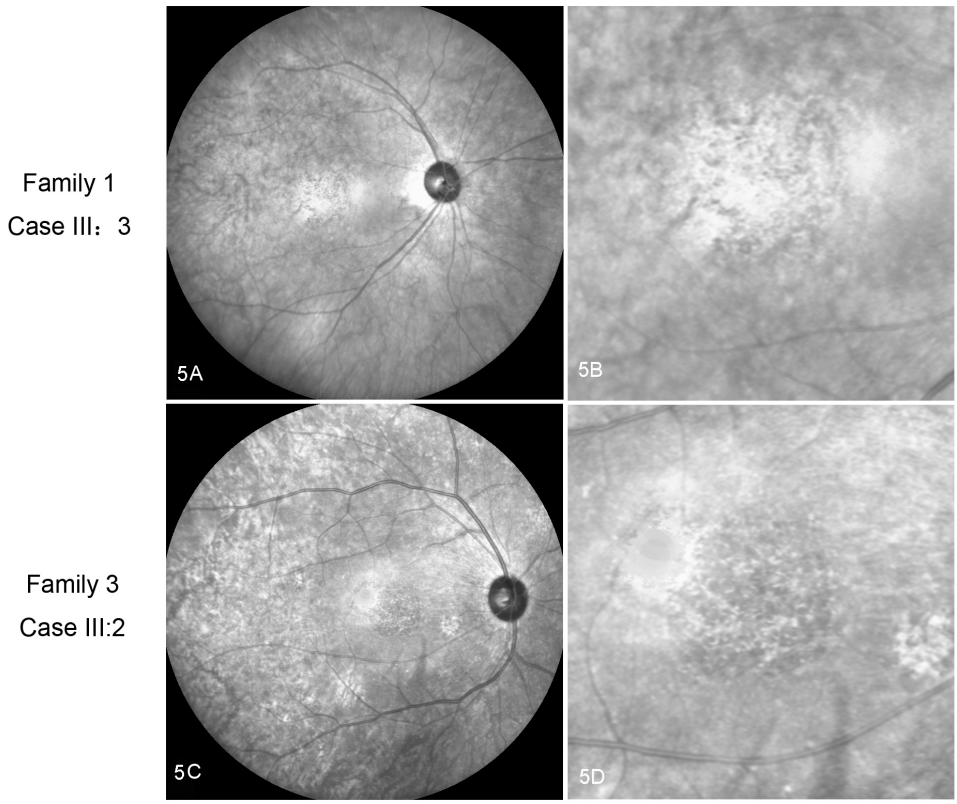

Figure 5. Photograph from the 633-nm laser of a scanning laser ophthalmoscope of patients with variants in *AXTN7*. A coarse granular appearance was observed in Family 1 Case III:3 (a 54-year-old woman, right eye; **A**) and Family 3 Case III:2 (a 32-year-old man, right eye; **C**). A coarse granular appearance was observed in both patients. Panels **B** and **D** are enlargements of panels **A** and **C**.

−0.5−1.0 × 85 OS. No specific abnormality was found on the fundus examination (Figure 2G,H). However, OCT showed mild thinning of the macula and atrophic changes in the RPE and the ellipsoid zone. A reduction of central responses was demonstrated on multifocal ERGs.

Family 3: A 32-year-old man (Case III:2) reported decreased visual acuity, hemeralopia, and photophobia at age 28 and gait disturbance at age 30. Computed tomographic scans and magnetic resonance images showed cerebellar atrophy. His BCVA was 0.1 OU with a refraction of −0.5−0.5 × 15 OD and −0.5 OS. The anterior segment examination was normal.

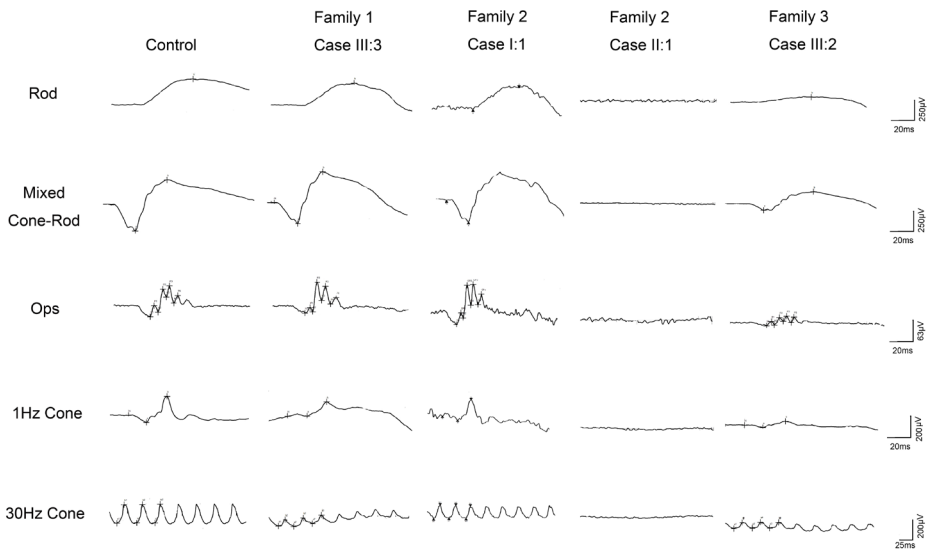

Figure 6. Standard ERGs in patients with variants in *AXTN7*. Representative rod, mixed cone-rod, and cone electroretinograms (ERGs) from the patients compared with a healthy subject.

The fundus examination revealed pigmentary changes in the macular area (Figure 2I,J), which corresponded to the AF hypofluorescence patch in a rounded square shape with a surrounding hyperfluorescent ring (Figure 3E,F). OCT showed macular atrophy, extreme thinning of the fovea, and many hyperreflective dots (Figure 4K–N). VF analysis confirmed a central scotoma in both eyes. The ERGs presented severely decreased cone-rod responses (Figure 6). The pathological allele carried 48 CAG repeats. His son (IV:1) was a 4-year-old boy who began to be unable to walk and pursue objects at age 2. He was bedridden with respiratory failure and lost light perception at age 4. He was confirmed with gene testing, with CAG repeats of 113.

The results of the clinical characterization and genetic tests of all patients are summarized in Table 1. The CAG repeat numbers of the 30 healthy controls were $(CAG)_7$ (6/60, 10.0%), $(CAG)_{10}$ (41/60, 68.3%), $(CAG)_{11}$ (2/60, 3.3%), and $(CAG)_{12}$ (11/60, 18.3%).

DISCUSSION

SCA7 is a form of SCA with a proportion of 2.00%–26.6% in different regions worldwide [13-18], with a prevalence of around 1/500,000 [19]. SCA7 is the most common autosomal dominant ataxia in Sweden, Norway, Denmark, and Finland as a result of the founder effect [17]. In the Chinese population, SCA3 has been reported as the most common subtype of SCAs (54.6%), and SCA7 accounts for only 4.80% of SCAs [18]. In patients with SCA7, the unstable expanded trinucleotide repeats of CAG induce a cytotoxic gain of function of ataxin-7. It localizes to the nucleus or the cytoplasm or both depending on the cell population and is widely expressed in human tissues [20,21]. In the retina, ataxin-7 is present in all neurons located in the nuclei and inner segments of photoreceptors and absent in their outer segments [2]. The expression of polyQ-ataxin-7 in *AXTN7* has been known to cause the cellular loss of specific neuronal cells, including retinal photoreceptors, through a toxic effect that causes downregulation of the genes involved in phototransduction, development, and differentiation of photoreceptors [22]. Moreover, it was reported that cytoplasmic ATXN7 is associated with microtubules (MTs) [23]. Although the polyQ sequence in *ATXN7* is not essential for the interaction with MTs, polyQ-expanded ATXN7 in the inner segments could engage in inappropriate with cofactors whose dysregulation might affect intracellular protein trafficking, organelle delivery, or axonal transport pathways.

The size of the pathogenic CAG repeats in *ATXN7* is inversely correlated with the age of onset of symptoms and the rate of disease progression [1,2,19,24]. Patients with SCA7 have been reported to have 37–460 CAG repeats compared with the four to 35 CAG repeats in the normal allele [1,18,25,26], with the earliest onset during infancy [27]. The number of pathological CAG repeats in the study patients was 43−113, and ten CAG repeats was the most common in the Chinese population. In this cohort, patients with 43–45 CAG repeats were in their 40s at the age of onset, patients with 48–50 repeats were their 20s at the age of onset, and for patients with 56–62 CAG repeats, symptoms began during their teenage years. If the number of CAG repeats reached more than 100, symptoms began in childhood and worsened rapidly, thus making them life-threatening. With relatively fewer CAG repeats, patients could be asymptomatic. For example, Family 2 Case II:1 (45 CAG repeats) had no complaints when he was 38, and clinical examination revealed no obvious abnormality in the retina. During the 4-year follow-up, we noticed gradually progressing cone dysfunction, which did not affect his normal life. Park et al. [10] reported a case of a 52-year-old woman who presented with a lower number (38) of CAG repeats in *ATXN7* and a mild form of retinal degeneration, which was similar to the classic type of OMD. However, in this case, the follow-up period lasted only 8 months. It is possible that this case would develop to cone-rod dystrophy over the next few years. OMD is a certain stage for these patients with a lower number of CAG repeats. Conversely, the phenotype in patients with more than 100 CAG repeats could be severe. For example, the youngest patient in the present study, Family 3 Case IV:1, with 113 CAG repeats exhibited severe vision loss and dyskinesia, and he deteriorated rapidly within 2 years. The present findings are consistent with those in the literature in that long expansion associated with infantile-onset SCA7 occurs exclusively in paternal transmission [11]. This phenomenon underscores the exceptional instability of *AXTN7* CAGs in male meiosis. Such instability was confirmed by genotyping the individual sperm of SCA7 males carrying 46 or 53 CAGs [28].

Clinically, visual disturbances may precede other symptoms in SCA7. Multimodal imaging may facilitate the observation of retinal change and is beneficial for detecting early lesions of *ATXN7*-related retinopathy. The retinal phenotype in the study patients indicating cone-rod dystrophy generally agrees with that in previous reports [1,8-11]. In the present cohort, all the patients complained of progressive bilateral visual loss, and most cases reported visual disturbance earlier than dyskinesia or dysarthria. The severity of retinopathy can vary from a normal retina appearance to severe cone-rod dystrophy, and it is correlated with the number of CAG repeats and age. The thinning of the macular tissue on OCT and the dark macular area on AF demonstrated the severity

Molecular Vision 2021; 27:221-232 <http://www.molvis.org/molvis/v27/221>

Table 1. The clinical characterization and genetic test of patients with SCA7.

Family No.	Patient No.	Age (y)	Sex	Age at onset Ophthalmol	Age at onset cerebellar	Expanded repeat	Normal repeat	BCVA OD	BCVA OS	OCT	VF	AF	ERGs
1	Case III:3	54	F	45	51	≈45	10	0.1	0.1	Macular atrophy with hyperreflective dots	Central scotoma	Dark macular with hyperfluorescent ring	Severely decreased cone responses with preserved rod function
	Case III:9	57	M	40s	40s	≈43	10	NA	NA	NA	NA	NA	NA
	Case IV:5	32	M	26	30	≈50	10	0.4	0.32	NA	NA	NA	Severely decreased cone responses with preserved rod function
	Case IV:4	26	M	Teenage	18	≈56	10	HM	HM	NA	NA	NA	NA
2	Case II:1	14	F	12	13	≈62	10	0.1	0.08	Macular atrophy with hyperreflective dots	Central scotoma	Dark macular with hyperfluorescent ring	Severely decreased cone responses with a little preserved rod function (age 14). Extinguished (age 18)
	Case I:1	38	M	39	40s	≈45	10	0.1(age 42)	0.1(age 42)	Normal(age 38)	NA	NA	Normal (age 38)
3	Case III:2	32	M	28	30	≈48	10	0.1	0.1	Macular atrophy with hyperreflective dots	Central scotoma	Dark macular with hyperfluorescent ring	Severely decreased cone and rod responses
	Case IV:1	4	M	2	2	≈113	6	NLP	NLP	NA	NA	NA	NA

and the area of macular dystrophy, including diffuse or local photoreceptor degeneration and disruption of the RPE. The thinning of the RPE on OCT might be attributable to photoreceptor damage and RPE loss caused by metabolic burden. Compared with Stargardt macular dystrophy, the shape of the hypofluorescent area in the macula could be round, petal-like, and a rounded square, while it is a horizontal oval in Stargardt macular dystrophy [29]. In some patients, we observed a hyperfluorescent ring around a dark macula on AF, indicating the expansion of the macular atrophy. Abnormalities in the ERGs tend to be more prominent in cone-mediated responses or in cone and rod signals, which are the features of an evolving cone-rod dystrophy depending on the stage of the disease and the number of CAG repeats. We also noticed that in Family 2 Case II:1, the ERGs evolved from residual weak rod responses to extinguished within the 4-year follow-up.

We observed a common sign of OCT in the patients in the advanced stage, that is, hyperreflective dots in the outer retinal layers, the number of which decreases in the late stage. We reviewed an OCT scan in a patient with SCA7 reported previously and found that the hyperreflective dots could also be easily identified [19], indicating that this appearance could be an OCT feature for patients with SCA7. The hyperreflective dots seemed to correspond to the coarse granular appearance on the 633-nm laser SLO, but they were not visible on the fundus photograph or AF. The hyperreflective dots were not seen in patients at the early stage (Family 2 Case II:1), and patients at the late stage had fewer dots (Family 2 Case I:1), indicating a lesion at a certain stage of the disease. Furthermore, the dots tended to accumulate at the border of a dystrophic retina and a relatively normal retina. Polyglutamine expansion in *ATXN7* causes its misfolding and prominent intranuclear accumulation, disrupting a wide range of cellular processes and finally, leading to the death of photoreceptors [30]. The hyperreflective dots were likely the degenerative photoreceptors or macrophages that have ingested degenerative photoreceptors, reflecting the phagocytosis of photoreceptor outer segments. The dense hyperreflective dots in the choroidal vessel layers are also observed in other retinal diseases, such as Stargardt disease [31] and central serous chorioretinopathy [32]. The present study clearly demonstrates that the hyperreflective dots are more prevalent in the choroidal layers, specifically in the Bruch membrane/RPE complex and choriocapillaris. The reason for the presence of hyperreflective foci in the choroid is uncertain. The cause of the retinal and neuronal dysfunction and how it is related to the polyglutamine repeat is not yet fully understood.

In this study, we also improved the molecular diagnostic method for testing patients with SCA7. We used simultaneous Sanger sequencing for homozygous individuals to calibrate the CAG expansions of the fluorescence PCR. Fluorescence PCR and capillary electrophoresis for the detection of dynamic mutations, such as *ATXN7*, have the advantages of being simple, fast, and cost-effective. However, this method should be used to guard against false-negative results, and it should be used with other methods, such as Southern blotting.

In summary, we provided a detailed retinal study on patients with SCA7, which could be considered cone-rod dystrophy. We also noted an important feature, that is, hyperreflective dots, on OCT and improved the molecular diagnostic method of SCA7. The case series illustrates that multimodal imaging of the retina is beneficial for detecting early lesions of cone-rod dystrophy related to SCA7, and that this type of imaging could help ophthalmologists produce a specific diagnosis.

ACKNOWLEDGMENTS

This study was supported by the Fundamental Research Funds for the Central Universities (3332020015), Youth Program of Peking Union Medical College Hospital (pumch201911263), National Natural Science Foundation of China (81873687) and CAMS Innovation Fund for Medical Sciences of China (CIFMS 2016–12M-1–002). Availability of data and material: The data sets used and/or analyzed during the current study are available from the corresponding author on reasonable request.

REFERENCES

1. Atadzhanov M, Smith DC, Mwaba MH, Siddiqi OK, Bryer A, Greenberg LJ. Clinical and genetic analysis of spinocerebellar ataxia type 7 (SCA7) in Zambian families. Cerebellum Ataxias 2017; 4:17-[PMID: 29214039].
2. Niewiadomska-Cimicka A, Trottier Y. Molecular Targets and Therapeutic Strategies in Spinocerebellar Ataxia Type 7. Neurotherapeutics 2019; 16:1074-96. [PMID: 31432449].
3. Jin DK, Oh MR, Song SM, Koh SW, Lee M, Kim GM, Lee WY, Chung CS, Lee KH, Im JH, Lee MJ, Kim JW, Lee MS. Frequency of spinocerebellar ataxia types 1,2,3,6,7 and dentatorubral pallidoluysian atrophy mutations in Korean patients with spinocerebellar ataxia. J Neurol 1999; 246:207-10. [PMID: 10323319].
4. Pogacar S, Ambler M, Conklin WJ, O'Neil WA, Lee HY. Dominant spinopontine atrophy. Report of two additional members of family W. Arch Neurol 1978; 35:156-62. [PMID: 629660].
5. Jardim LB, Pereira ML, Silveira I, Ferro A, Sequeiros J, Giugliani R. Machado-Joseph disease in South Brazil: clinical and

molecular characterization of kindreds. Acta Neurol Scand 2001; 104:224-31. [PMID: 11589651].

6. Sun YM, Lu C, Wu ZY. Spinocerebellar ataxia: relationship between phenotype and genotype - a review. Clin Genet 2016; 90:305-14. [PMID: 27220866].

7. Miller RC, Tewari A, Miller JA, Garbern J, Van Stavern GP. Neuro-ophthalmologic features of spinocerebellar ataxia type 7. J Neuroophthalmol 2009; 29:180-6. [PMID: 19726938].

8. Abe T, Tsuda T, Yoshida M, Wada Y, Kano T, Itoyama Y, Tamai M. Macular degeneration associated with aberrant expansion of trinucleotide repeat of the SCA7 gene in 2 Japanese families. Arch Ophthalmol 2000; 118:1415-21. [PMID: 11030825].

9. Aleman TS, Cideciyan AV, Volpe NJ, Stevanin G, Brice A, Jacobson SG. Spinocerebellar ataxia type 7 (SCA7) shows a cone-rod dystrophy phenotype. Exp Eye Res 2002; 74:737-45. [PMID: 12126946].

10. Park JY, Wy SY, Joo K, Woo SJ. Spinocerebellar ataxia type 7 with RP1L1-negative occult macular dystrophy as retinal manifestation. Ophthalmic Genet 2019; 40:282-5. [PMID: 31269856].

11. Michalik A, Martin JJ, Van Broeckhoven C. Spinocerebellar ataxia type 7 associated with pigmentary retinal dystrophy. European journal of human genetics Eur J Hum Genet 2004; 12:2-15. [PMID: 14571264].

12. McCulloch DL, Marmor MF, Brigell MG, Hamilton R, Holder GE, Tzekov R, Bach M. ISCEV Standard for full-field clinical electroretinography (2015 update). Doc Ophthalmol 2015; 130:1-12. [PMID: 25502644].

13. Bryer A, Krause A, Bill P, Davids V, Bryant D, Butler J, Heckmann J, Ramesar R, Greenberg J. The hereditary adult-onset ataxias in South Africa. J Neurol Sci 2003; 216:47-54. [PMID: 14607302].

14. Smith DC, Bryer A, Watson LM, Greenberg LJ. Inherited polyglutamine spinocerebellar ataxias in South Africa. S Afr Med J 2012; 102:683-6. [PMID: 22831947].

15. Garcia-Velazquez LE, Canizales-Quinteros S, Romero-Hidalgo S, Ochoa-Morales A, Martinez-Ruano L, Marquez-Luna C, Acuna-Alonzo V, Villarreal-Molina MT, Alonso-Vilatela ME, Yescas-Gomez P. Founder effect and ancestral origin of the spinocerebellar ataxia type 7 (SCA7) mutation in Mexican families. Neurogenetics 2014; 15:13-7. [PMID: 24374739].

16. Storey E, du Sart D, Shaw JH, Lorentzos P, Kelly L, McKinley Gardner RJ, Forrest SM, Biros I, Nicholson GA. Frequency of spinocerebellar ataxia types 1, 2, 3, 6, and 7 in Australian patients with spinocerebellar ataxia. Am J Med Genet 2000; 95:351-7. [PMID: 11186889].

17. Jonasson J, Juvonen V, Sistonen P, Ignatius J, Johansson D, Bjorck EJ, Wahlstrom J, Melberg A, Holmgren G, Forsgren L, Holmberg M. Evidence for a common Spinocerebellar ataxia type 7 (SCA7) founder mutation in Scandinavia. European journal of human genetics Eur J Hum Genet 2000; 8:918-22. [PMID: 11175279].

18. Wang J, Xu Q, Lei L, Shen L, Jiang H, Li X, Zhou Y, Yi J, Zhou J, Yan X, Pan Q, Xia K, Tang B. [Studies on the CAG repeat expansion in patients with hereditary spinocerebellar ataxia from Chinese Han]. Zhonghua yi xue yi chuan xue za zhi = Zhonghua yixue yichuanxue zazhi = Zhonghua Yi Xue Yi Chuan Xue Za Zhi 2009; 26:620-5. [PMID: 19953482].

19. Niu C, Prakash TP, Kim A, Quach JL, Huryn LA, Yang Y, Lopez E, Jazayeri A, Hung G, Sopher BL, Brooks BP, Swayze EE, Bennett CF, La Spada AR. Antisense oligonucleotides targeting mutant Ataxin-7 restore visual function in a mouse model of spinocerebellar ataxia type 7. Sci Transl Med 2018; 10:eapp8677[PMID: 30381411].

20. Einum DD, Townsend JJ, Ptacek LJ, Fu YH. Ataxin-7 expression analysis in controls and spinocerebellar ataxia type 7 patients. Neurogenetics 2001; 3:83-90. [PMID: 11354830].

21. Lindenberg KS, Yvert G, Muller K, Landwehrmeyer GB. Expression analysis of ataxin-7 mRNA and protein in human brain: evidence for a widespread distribution and focal protein accumulation. Brain Pathol 2000; 10:385-94. [PMID: 10885657].

22. Abou-Sleymane G, Chalmel F, Helmlinger D, Lardenois A, Thibault C, Weber C, Merienne K, Mandel JL, Poch O, Devys D, Trottier Y. Polyglutamine expansion causes neurodegeneration by altering the neuronal differentiation program. Hum Mol Genet 2006; 15:691-703. [PMID: 16434483].

23. Nakamura Y, Tagawa K, Oka T, Sasabe T, Ito H, Shiwaku H, La Spada AR, Okazawa H. Ataxin-7 associates with microtubules and stabilizes the cytoskeletal network. Hum Mol Genet 2012; 21:1099-110. [PMID: 22100762].

24. Sequeiros J, Martindale J, Seneca S, Giunti P, Kamarainen O, Volpini V, Weirich H, Christodoulou K, Bazak N, Sinke R, Sulek-Piatkowska A, Garcia-Planells J, Davis M, Frontali M, Hamalainen P, Wieczorek S, Zuhlke C, Saraiva-Pereira ML, Warner J, Leguern E, Thonney F, Quintans Castro B, Jonasson J, Storm K, Andersson A, Ravani A, Correia L, Silveira I, Alonso I, Martins C, Pinto Basto J, Coutinho P, Perdigao A, Barton D, Davis M. EMQN Best Practice Guidelines for molecular genetic testing of SCAs. European journal of human genetics Eur J Hum Genet 2010; 18:1173-6. [PMID: 20179742].

25. Durr A. Autosomal dominant cerebellar ataxias: polyglutamine expansions and beyond. Lancet Neurol 2010; 9:885-94. [PMID: 20723845].

26. Takahashi T, Katada S, Onodera O. Polyglutamine diseases: where does toxicity come from? what is toxicity? where are we going? J Mol Cell Biol 2010; 2:180-91. [PMID: 20410236].

27. Benton CS, de Silva R, Rutledge SL, Bohlega S, Ashizawa T, Zoghbi HY. Molecular and clinical studies in SCA-7 define a broad clinical spectrum and the infantile phenotype. Neurology 1998; 51:1081-6. [PMID: 9781533].

28. Monckton DG, Cayuela ML, Gould FK, Brock GJ, Silva R, Ashizawa T. Very large (CAG)(n) DNA repeat expansions in the sperm of two spinocerebellar ataxia type 7 males. Hum Mol Genet 1999; 8:2473-8. [PMID: 10556295].

29. Sun Z, Yang L, Li H, Zou X, Wang L, Wu S, Zhu T, Wei X, Zhong Y, Sui R. Clinical and genetic analysis of the ABCA4 gene associated retinal dystrophy in a large Chinese cohort. Exp Eye Res 2021; 202:108389-[PMID: 33301772].

30. La Spada AR, Taylor JP. Repeat expansion disease: progress and puzzles in disease pathogenesis. Nat Rev Genet 2010; 11:247-58. [PMID: 20177426].

31. Piri N, Nesmith BL, Schaal S. Choroidal hyperreflective foci in Stargardt disease shown by spectral-domain optical coherence tomography imaging: correlation with disease severity. JAMA Ophthalmol 2015; 133:398-405. [PMID: 25590640].

32. Hanumunthadu D, Matet A, Rasheed MA, Goud A, Vuppurabina KK, Chhablani J. Evaluation of choroidal hyperreflective dots in acute and chronic central serous chorioretinopathy. Indian J Ophthalmol 2019; 67:1850-4. [PMID: 31638047].

Articles are provided courtesy of Emory University and the Zhongshan Ophthalmic Center, Sun Yat-sen University, P.R. China. The print version of this article was created on 7 May 2021. This reflects all typographical corrections and errata to the article through that date. Details of any changes may be found in the online version of the article.